

# Grasp Selection for In-Hand Robotic Manipulation of Non-Rigid Objects with Shape Control

Félix Nadon, Pierre Payeur  
*School of Electrical Engineering and Computer Science*  
*University of Ottawa*  
Ottawa, Canada  
[fnado079, ppayeur]@uottawa.ca

**Abstract**—The ability to intelligently manipulate non-rigid objects with a robotic hand is a requirement for many tasks which remain to be automated in domains such as agriculture, food processing, or medicine. This ability includes the nontrivial skill of controlling the shape of the object during the manipulation, which normally requires advanced knowledge of the properties of the object under manipulation as well as simulation capabilities. This work proposes an efficient algorithm and control framework that integrates RGB-D computer vision with a three-finger robotic gripper in a systemic approach for selecting the initial grasp points for a 2D shape control task through visual inspection of the object and desired target shape contours.

**Index Terms**—grasp selection; shape control; non-rigid objects; robotic manipulation;

## I. INTRODUCTION

The intelligent manipulation of non-rigid objects by robotic systems is a prerequisite for automating a variety of delicate or labour-intensive tasks in industries such as agriculture, food processing, medicine, and response to natural disasters. However, as shown in recent surveys [1, 2], robotic manipulation of such objects has not progressed far beyond linear (ropes) and planar (cloth) objects. In particular, most research considering 3D objects or their 2D projections (contours) starts with predefined, rigid contacts between the manipulator(s) and the object. This research improves and expands on our previous work on grasp selection [3] by using a more accurate hand model, improved contour tracking, and a formal validation of force closure.

The manipulation task considered in this research is the reshaping of a non-rigid object’s 2D contour so that it comes as close as possible to an arbitrarily defined target contour. While there are some immediate applications resembling this task (such as inserting a foam filter in a rigid enclosure), the main interest is to explore the fundamental issue of in-hand shape control, which is involved to some extent in any dexterous manipulation of non-rigid objects. In particular, the problem addressed here is the selection of the grasp points that will allow to complete the reshaping task efficiently while respecting the constraints imposed by the robotic manipulator and grasp stability. A simple approach to solve this would be to sample all possible grasps and evaluate their quality in terms of their stability and ability to complete the task. Depending on the sampling factor and on the geometry of the selected robotic hand, this could lead to a large number of grasps to evaluate

and may require a significant amount of time. In scenarios where online grasp selection is required, it is justified to use a more elaborate procedure to eliminate the grasps that do not allow the desired reshaping or that are unstable as quickly as possible.

The rest of this paper is organized as follows: section II provides a brief overview of the related literature. Section III details the proposed approach, including the experimental setup (III-A), modeling of the robotic hand and camera (III-A1 and III-A2), system architecture (III-B), task definition (III-C) as well as the proposed grasp selection algorithm (III-D to III-F). Finally, section IV analyses a sample of results while section V provides concluding remarks and future directions.

## II. RELATED LITERATURE

The grasp selection problem may be described as the distribution of the contact points between the robotic manipulator(s) and the surface (or contour, in the 2D case) of the manipulated object in a way that will create a stable grasp and allow to complete the desired task while maintaining the object’s structural integrity. While humans are able to intuitively select such a grasp for a variety of objects and tasks, it is not a trivial problem to solve for robotic systems, especially with the additional complexity of non-rigid objects.

Generating a stable grasp is a well known topic for rigid objects [4, 5], with the three main paradigms being model-based, heuristic, and learning approaches. Model-based techniques such as [6, 7] rely on a mathematical description of the object to build an analytical description of all possible grasps. This function is then optimized based on the mathematical criteria imposed by the task to perform. Heuristic approaches such as [8, 9] avoid the need for curve-fitting algorithms by working directly with sensor data, such as a list of contour points in an image. They perform a search along the object contour to optimize some criteria related to grasp quality, such as curvature or symmetry. Finally, many of the more recent approaches such as [10–12] prefer to use machine learning techniques with a database of objects and grasps to identify which grasps are possible for a given object.

The selection of a stable grasp for in-hand manipulation of non-rigid objects has not yet been widely addressed. Some works on this topic include Gopalakrishnan and Goldberg [13], who discuss the concept of “deform closure” in the 2D case,

a scenario which is equivalent to holding a similarly-shaped rigid object in form closure with contact points in concavities. Mira et al. [14] study the scenario where it is impossible to form a force closure grasp without deforming the object, such as a sheet of paper lying on a table. They generate grasps with a learning system and a database of objects with successful and failed grasps. Zaidi et al. [15, 16] use a model-based approach to generate stable grasps on non-rigid objects with a three-fingered robotic hand. They accomplish this by fitting grasp polygons around the object model to validate the force closure constraints before simulating the hand-object interaction to determine the forces necessary to reach stability while minimizing object deformation.

### III. GRASP SELECTION

#### A. Experimental Setup

The experimental setup used in this research is shown in Fig. 1 and consists of a Microsoft Kinect v1 for Xbox 360 mounted to obtain a view that is normal to the palm of a BH8-262 Barrett hand [17], which is placed on a table. The object to deform is placed on the hand alongside outlines of the desired target shapes toward which the reshaped object should converge. This experimental setup and the contour detection technique used require a few constraints on the experiment. The main requirements are that the object is sufficiently different in colour and texture from the background to be distinguished, and that it is well represented by its 2D projection (i.e., no significant protrusions or indentations at different depths). While it is not a hard requirement, the grasp selection algorithm also considers that the centre of the object is aligned with the centre of the hand. In order to compute the direction of the applied forces in the 2D plane as well as the pixels-to-mm conversion factor, it is necessary to construct simplified models of the Barrett hand and Kinect, which are formulated as follows:

1) *Barrett hand*: The BH8-262 Barrett hand is built with three identical fingers, one of which (F3) is in a fixed orientation while the two others can rotate around the palm, with an identical angle  $\phi$  between F3 and each of F1 and F2. In a 2D view which is normal to the palm, the paths of the fingers form straight lines which converge near the centre of the palm. However, there is a 25 mm offset between the center of the palm and the pivot points of fingers F1 and F2, which causes the convergence point of the finger paths to move colinearly with the path of F3 as the angle  $\phi$  varies. This situation is illustrated in Fig. 2. In order to accurately compute the directions of the forces applied by the fingers, it is necessary to know the location of the convergence point of the finger paths with respect to the centre of the palm. Given the angles  $\psi_1$  and  $\psi_2$  defined in Fig. 2, we look for  $y(\phi)$ , the distance along the path of F3 between the centre of the palm and the convergence point.

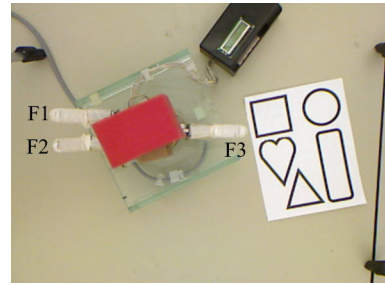
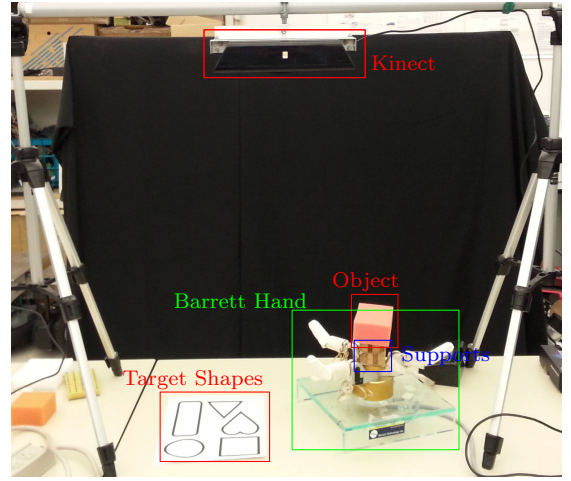


Fig. 1. (a) Experimental setup and (b) resulting view

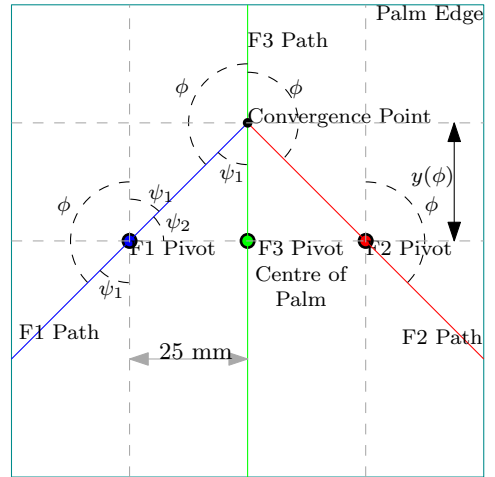


Fig. 2. The convergence point of the finger paths varies with  $\phi$

$$\begin{aligned} \tan(\psi_2) &= \frac{y(\phi)}{25 \text{ mm}} \\ \psi_2 &= 90^\circ - \psi_1 \\ \psi_1 &= 180^\circ - \phi \end{aligned} \quad (1)$$

Therefore,

$$y(\phi) = 25 \text{ mm} \cdot \tan(\phi - 90^\circ) \quad (2)$$

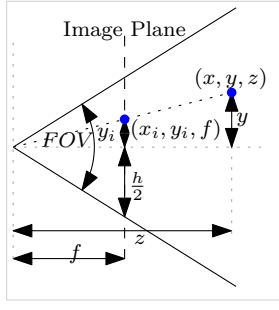


Fig. 3. Non-inverting pinhole camera model

2) *Kinect*: We use the classical non-inverting pinhole camera model shown in Fig. 3, where  $(x_i, y_i)$  are the coordinates of a point in the image plane and  $(x, y, z)$  are its coordinates with respect to the camera. Given that  $z$  is measured by the Kinect and that its field of view (FOV) and image size are known ( $48.6^\circ$  by  $62^\circ$  and  $480$  px by  $640$  px, vertically and horizontally [18]), it is possible to geometrically compute the position of a point in the world from its position in the image, as well as  $\gamma(z)$ , the conversion factor between pixels and millimetres. The development of (3) is identical in the  $x$  and  $y$  directions, which both lead to the same value of  $\gamma(z)$ .

$$\gamma(z) \text{ mm/px} = \frac{z \text{ mm}}{f \text{ px}} = \frac{z \text{ mm}}{\frac{h \text{ px}}{2 \tan(\frac{FOV}{2})}} = \frac{z}{532} \text{ mm/px} \quad (3)$$

### B. System Architecture

Because the shape and behaviour of non-rigid objects are not fixed but instead evolve during the manipulation, it is essential that their dexterous manipulation is done through a systemic approach that enables the integration and sharing of information between the different manipulation phases. Fig. 4 presents the robotic manipulation system that is developed in this research. It consists of three main steps/algorithms, namely the initialization, grasp selection, and shape control phases. These interact with three custom software modules that enable the interaction with the Kinect and Barrett hand and provide contour detection capabilities. While this paper focuses on the second phase, grasp selection, which is completely automated, some user interaction is required to identify the object and target shape in the initialization phase, as well as to align the hand with the selected grasp due to the absence of a mechanical wrist in the shape control phase.

### C. Manipulation Task Identification

The contour identification and tracking technique used in this research is the fast level-set algorithm in the log-polar domain [19]. As shown in Fig. 5a, the primary advantage of the log-polar transformation is that the object contour separates the image vertically while ensuring that the object occupies a larger portion of the image than the background. These properties accelerate the convergence of the fast level-set algorithm, which relies on the permutation of pixels between the “inside” and “outside” of the object based on their colour statistics.

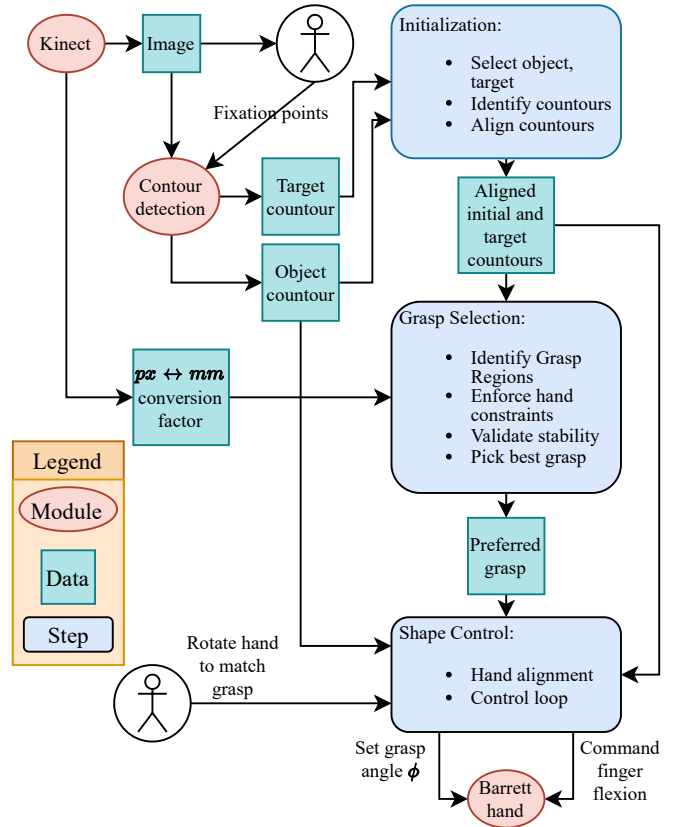


Fig. 4. Overview of the robotic manipulation system

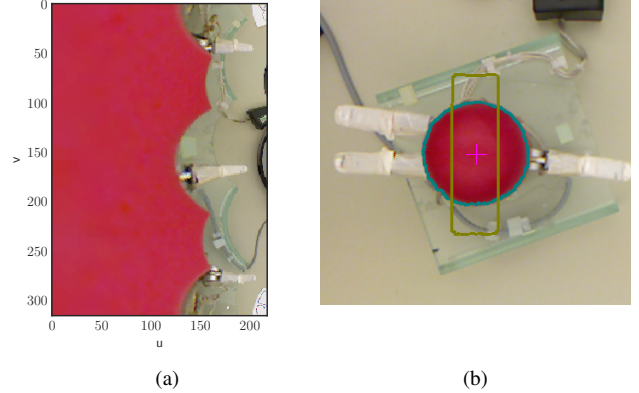


Fig. 5. (a) Log-polar image transform on the red sponge shown in Fig. 1b and (b) definition of the reshaping task: the initial object contour (blue) should be deformed to match the target contour (gold) as closely as possible

In this work, the initial depth-filtering of the point cloud proposed in [19] is replaced by a simpler approach to locate the object. Initially, the input picture is converted to the log-polar domain with a very low sampling rate, which allows to quickly execute the fast level-set algorithm to identify the boundaries of the object. The input image may then be cropped to these boundaries, reducing the number of points to process when applying the algorithm to a high-resolution image to find and track the precise object contour.

Given the initial view shown in Fig. 1b, the reshaping task

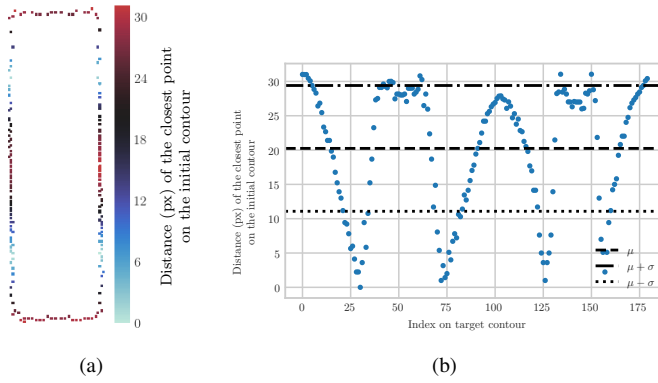


Fig. 6. Visualization of the distance between the initial and target contours shown in Fig. 5b as (a) a map projected on the target contour, and (b) a graph with its mean  $\mu$  and standard deviation  $\sigma$

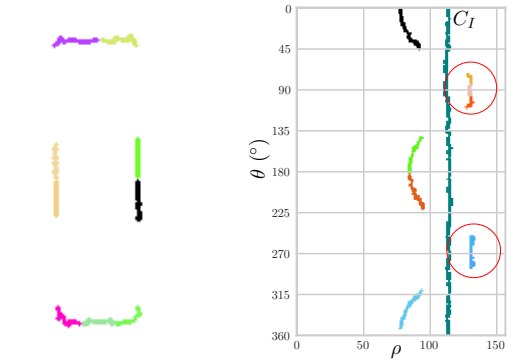
to perform is defined by selecting a point on the object and a point inside one of the target contours. These are used as focal points for the log-polar fast level-set algorithm which allows to identify both contours. Image moment analysis [20] is then used on the binary images corresponding to the filled contours to identify the centroid and main axis of both the object and target. These parameters are used to automatically align the target contour over the object, thereby defining the reshaping task as shown in Fig. 5b. We note that the target contour must also be scaled by a factor of  $\frac{\gamma_{object}}{\gamma_{target}}$  to compensate for the height difference between where the object and target shapes are imaged.

#### D. Grasp Regions Identification

According to the principle of diminishing rigidity [21], the influence of the forces applied by a robotic hand on the manipulated object is maximal at the contact points between the object and fingers, and this influence diminishes as the distance between a considered point and the contact point increases. It follows that the contact points should be positioned in the areas where the influence of the applied forces is to be maximized. In the context of 2D shape control of a non-rigid object, these are the areas where there is a large distance between the initial contour of the object and the desired target contour. Fig. 6 shows, for a sample reshaping task, the distance between the initial and desired contours, projected on the desired contour.

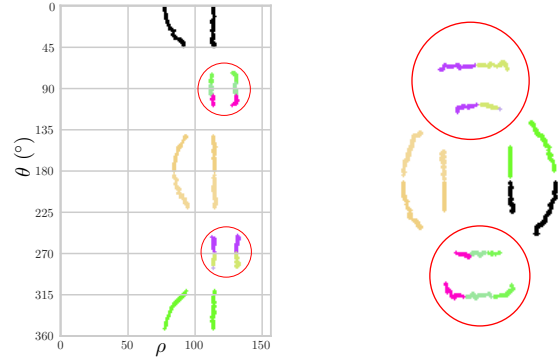
Empirically, an appropriate threshold for selecting contact points is the mean of the initial distance. That is, only the regions where the distance between the initial and target contours is larger than the mean are considered for grasping. These regions are then subdivided in continuous sub-regions, identified with different colours in Fig. 7a, that match the width of the robotic fingers.

Since the grasping regions have been identified on the target contour only, it is necessary to associate them with the corresponding regions on the initial object contour. Because the general direction of the finger motion is towards the centre of the hand, it is possible to take advantage of polar coordinates to simplify this task. The initial and target contours are converted to a polar coordinate system centred on the



(a) Regions of interest for grasping on the target contour

(b) Initial object contour  $C_I$  and potential grasp regions of the target contour, in polar coordinates



(c) Association of regions between the target and initial contours, in polar coordinates

(d) Association of regions between the target and initial contours, in Cartesian coordinates

Fig. 7. Association of regions between the target and initial contours. Each “initial” region is set to the same colour as its matching “target” region. In the circled regions, the target contour is further from the centre of the hand than the initial contour. These are therefore ignored for grasp selection

centre of the palm. In this representation, all regions span a different interval of angles, such that the association may be completed by simply selecting the points of the initial contour that span the same interval of angles. Fig. 7b and Fig. 7c illustrate this process. As the fingers are not rigidly attached to the object, it is only possible to push on the contour to bring it closer to the centre of the hand. Because of this constraint, the regions where the target contour is further from the centre of the hand than the initial contour (i.e., it would be necessary to pull on the object) are eliminated from the process. The result is shown in the Cartesian domain in Fig. 7d.

The second step of grasp selection is to generate potential grasps based on the identified regions. In this step, two of the Barrett hand constraints are considered: the number of fingers and the necessity to have an identical angle ( $\phi$  in Fig. 2) between F3 and the two other fingers. Therefore, for every combination of three identified regions from the target contour, we must verify that it is possible to place a finger in each region while ensuring that the angle between one of them (F3) and the two others are similar. In order to validate this condition, the centre of the hand is once again used as an approximation for the convergence of the finger paths and

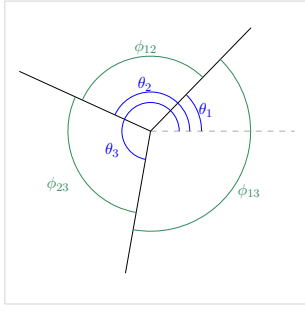


Fig. 8. Potential finger paths towards the object centre defined by the angles  $(\theta_1, \theta_2, \theta_3)$  in a polar representation. Black lines are interchangeably associated with the central finger F3. This is a valid grasp for the Barrett hand only if at least two of the internal  $\phi_{ij}$  angles are identical

the three regions are converted to a polar coordinate system centred on this point. With  $\theta_1, \theta_2, \theta_3$  as the central angles of the three regions considered and  $\tau$  as half of the angle range of the largest region, Algorithm 1, which is illustrated by Fig. 8, verifies the Barrett hand constraints and outputs  $\Theta_c$ , the direction of the central finger, and  $\phi$ , the grasp angle between F3 and the other two fingers. Thus, F3 is associated to the contour region containing  $\Theta_c$ , F1 is associated to the contour region containing  $\Theta_c - \phi$ , and F2 is associated to the contour region containing  $\Theta_c + \phi$ . The combination of  $\Theta_c$ ,  $\phi$  and the convergence point of the finger paths (which is for the moment approximated as the centre of the object) is sufficient to completely define a grasp with the Barrett hand in the context of shape control in a 2D space.

---

**Algorithm 1** Identifying valid grasps for the Barrett hand

---

**Input:**  $T = (\theta_1, \theta_2, \theta_3)$ , angles describing potential finger paths;  $\tau$ , the tolerance for internal angles equality  
**Output:**  $\Theta_{cidx}$ , the central angle;  $\phi$ , the difference between the central angle and the two others **if** the grasp is valid, **false** otherwise.  
**for**  $i \leftarrow 1 \dots 3$  **do**  
    **for**  $j \leftarrow i \dots 3$  **do**  
         $\phi_{ij} \leftarrow |\theta_i - \theta_j|$   
        **if**  $\phi_{ij} > 180^\circ$  **then**  
             $\phi_{ij} \leftarrow 360^\circ - \phi_{ij}$   
     $\Phi' \leftarrow (|\phi_{12} - \phi_{13}|, |\phi_{12} - \phi_{23}|, |\phi_{13} - \phi_{23}|)$   
     $\Theta_{cidx} \leftarrow \text{ARGMIN}(\Phi')$   
    **if**  $\Phi'_{\Theta_{cidx}} < \tau$  **then**  
        **if**  $\Theta_{cidx} = 1$  **then**  
             $\phi \leftarrow \text{MEAN}(\phi_{12}, \phi_{13})$   
        **else if**  $\Theta_{cidx} = 2$  **then**  
             $\phi \leftarrow \text{MEAN}(\phi_{12}, \phi_{23})$   
        **else if**  $\Theta_{cidx} = 3$  **then**  
             $\phi \leftarrow \text{MEAN}(\phi_{13}, \phi_{23})$   
    **else**  
        **return false**  
 $\Theta_c \leftarrow T_{\Theta_{cidx}}$   
**return**  $\Theta_c, \phi$

---

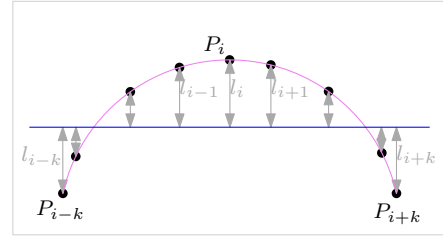


Fig. 9. Curvature by best-fit straight line: The curvature at point  $P_i$  is the mean of distances  $l$  between the contour and the blue straight line

**E. Stability Validation**

The stability of a grasp is validated in three steps, each evaluating a different criterion from simplest to most complex. First, grasps where  $\phi < 90^\circ$  do not respect the “vector closure” component of the force closure constraint. That is, the applied forces cannot have a sum of 0 with positive amplitudes, and therefore risk pushing the object out of the hand. Such grasps are considered unstable and eliminated from the process.

The second concern regarding grasp stability is minimizing the impact of finger positioning errors. As noted in [22], a stable grasp in a real-world manipulation scenario should be resistant to finger positioning errors. Indeed, while it is highly unlikely that the robotic fingers can be positioned exactly at the selected contact points due to limited mechanical and sensing accuracy, including the need for integer “pixel” coordinates throughout the process, such inaccuracies should not have a disproportionate impact on the stability and result of the grasp. One approach to ensure robustness is to avoid areas where the curvature of the object is significant [22, 23]. This is based on the observation that grasp points near sharp corners must be positioned more accurately than those in flatter areas in order to avoid errors. In this work, the technique used to compute the curvature of a grasp region is inspired by [9], who approximate the contour of the object by a series of straight lines. Here, the curvature around a point  $P_i$  is defined as the mean distance between all points from  $P_{i-k}$  to  $P_{i+k}$  and the best-fit straight line through those points (Fig. 9). Since the grasp regions are already defined to match the width of the robotic finger, the curvature is only evaluated at the central point of each region, taking the first and last points of the region as  $P_{i-k}$  and  $P_{i+k}$ , respectively. For each potential grasp, the curvature of the three grasp regions on the initial contour is evaluated and, if one of the curvatures is greater than an empirically determined threshold, the grasp is considered unstable and eliminated from the process. The sum of the three region curvatures of a grasp is used as a measure of the quality of the grasp.

The final step for validating grasp stability is to ensure that the fingers will not slip on the object. A practical approach to verify this condition is proposed by Morales et al. [8, 22] based on a model from Park and Starr [24]. This approach is based on the idea of “friction cones” created by the applied forces. To avoid slippage, it is necessary that the convergence point of the applied forces lie within the intersection of said friction cones. As shown in Fig. 10, this criteria may be simplified by verifying that the angle  $\beta$  between the applied

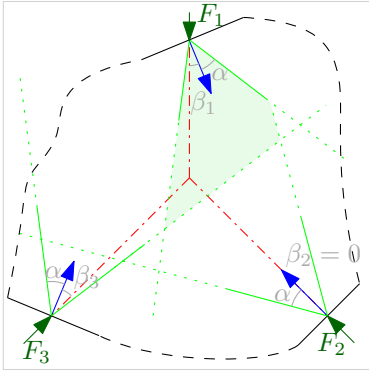


Fig. 10. To avoid slippage, the angle  $\beta_i$  between the applied force and the normal vector must be smaller than  $\alpha$

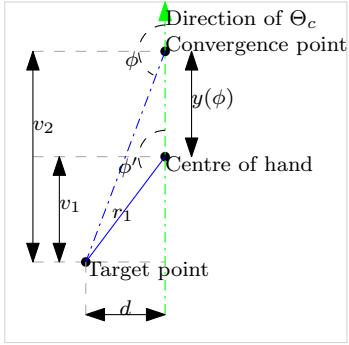


Fig. 11. Computing  $\phi$  from the path of F3 ( $\Theta_c$ ) and the position of another finger (target point)

force and the surface normal at the contact point is smaller than some parameter  $\alpha$ . This parameter could be computed with knowledge of the friction coefficient between the finger and the object or determined experimentally. In this work, a value of  $\alpha = 45^\circ$  was found to be sufficient.

In order to accurately validate the stability, it is necessary to compute the precise direction of the applied forces as well as their point of convergence, which was until now approximated as the centre of the object. Given an approximate grasp specified as three grasping regions, it is possible to take advantage of polar coordinates to compute both the proper spread angle  $\phi$  and the location of the forces convergence point from the direction of the central finger,  $\Theta_c$ , and a target point (in polar coordinates) on one of the two other regions. In a polar coordinates system centred on the centre of the hand, the contact point of F3 is defined as  $(r_c, \Theta_c)$  and the “target” point for the contact of F1 is  $(r_1, \theta_1)$ . Thus, the spread angle between the paths of F3 and F1 measured from the centre of the hand is also known as  $\phi' = \Theta_c - \theta_1$ . However, to match the geometry of the Barrett hand, this angle must be measured from the convergence point of the finger paths. This yields the geometry of Fig. 11, where we seek  $\phi$  and  $y(\phi)$ .

From Fig. 11, we know that

$$\phi' - 90^\circ = \arctan\left(\frac{v_1}{d}\right) \quad (4)$$

$$\phi - 90^\circ = \arctan\left(\frac{v_1 + y(\phi)}{d}\right) \quad (5)$$

Taking  $y(\phi)$  from (2) and applying the appropriate substitutions,

$$\begin{aligned} \phi - 90^\circ &= \arctan\left(\frac{v_1 + 25 \text{ mm} \cdot \tan(\phi - 90^\circ)}{d}\right) \\ d \tan(\phi - 90^\circ) &= v_1 + 25 \text{ mm} \cdot \tan(\phi - 90^\circ) \\ v_1 &= (d - 25 \text{ mm}) \tan(\phi - 90^\circ) \\ \phi - 90^\circ &= \arctan\left(\frac{v_1}{d - 25 \text{ mm}}\right) \end{aligned} \quad (6)$$

Since

$$d = r_1 \cos(\phi' - 90^\circ) \quad (7)$$

$$v_1 = r_1 \sin(\phi' - 90^\circ) \quad (8)$$

it is then possible to compute the correct  $\phi$  and  $y(\phi)$  based on the angle of finger F3 and a point in the grasp region of F1. For each combination of angle  $\Theta_c$  in the region associated with F3 and point in the region associated with F1, the above results are used to generate an accurate grasp for which to validate force closure.

Before computing the force closure condition, however, it is necessary to verify that the generated “accurate” grasp is still valid, i.e., that the finger paths intersect with the object contour. This verification is trivial in a polar coordinates system centred on the convergence point: we only need to verify that  $\Theta_c - \phi$  is in the angle interval of the grasp region associated with F2. Note that since the displacement of the convergence point is colinear with the path of F3, its intersection with the contour is not affected. Moreover, this is only computed for the initial object contour, as the change from approximate to accurate convergence point rarely preserves the intersections with the target contour, which is much closer to the centre of the polar projection. However, this does not seem to affect grasp stability. Once the validity of the grasp is confirmed, the force closure verification is completed by computing the angle between the applied force and the contour normal at the contact point. This normal is computed as a perpendicular vector to the best-fit straight line through the grasp region while the applied force is computed as the vector going from the intersection of the finger path and initial contour to the convergence point of the finger paths.

#### F. Selecting the Best Grasp

After the procedure detailed above, we obtain a list of stable grasps which respect the constraints of the Barrett hand while positioning the contact points in regions where there is a large distance between the initial and target contours. The final step of grasp selection is therefore to identify the grasp which best fulfills the different conditions detailed in this section. The principal criterion for selecting the preferred grasp is the positioning of the fingers in regions where the initial distance between the contours is large, thus we favour the grasp with the largest total distance between the initial and target contours (which the manipulation seeks to minimize). The secondary criteria are the mean angle between the applied

force and surface normal at the contact points on the initial and target contours (related to the quality of force closure), the total curvature of the grasp regions, and the mean distance between each contact point and the centre of the associated grasp region (to minimize the impact of positioning errors). These are used to break ties and avoid extreme cases.

Since grasp selection is highly dependant on the task at hand, it is useful to keep in mind that the goal of the manipulation is to deform the initial shape of object such that its contour comes as close as possible to the target shape. Therefore, the selected grasp will be much different than the one that would be selected to simply move the object (without considering its shape) or to perform some other tasks. Moreover, we note that the goal is not to select the optimal grasp in the strictest sense of the term, which would require a complete knowledge and simulation of the problem. It is rather to come close to the grasp that a human would intuitively select to perform the specified reshaping task given the constraints of the robotic hand.

#### IV. EXPERIMENTAL RESULTS

The proposed algorithm was tested in over 20 scenarios involving a variety of non-rigid objects and target shapes [25]. Fig. 12 presents a sample of selected grasps and the final deformed contours obtained with a controller based on the principle of diminishing rigidity [21] with real-time visual feedback. While this controller is not optimal for a 2D shape control task, it shows that the grasp remains stable and is able to bring the object’s contour closer to the desired shape. In general, we note that the selected grasp is close to the one that would be intuitively selected by a human given the detected contours, which may have artifacts and inaccuracies due to the reliance on contrast between the object and background for their detection. In Fig. 12a, we note a tendency to align the contours by the corners instead of by the sides, leading to a slight offset from the intuitive grasp (which would be perpendicular to the shortest sides of the sponge). We also note that the heart target shape in Fig. 12b is particularly interesting for testing and evaluating the grasp selection algorithm, as its well-defined concavity creates an area with a large distance from the more convex objects and naturally draws a contact point towards it, in addition to providing an easily recognizable “intuitive” grasp. Fig. 12c shows the case where the target shape is larger than the object in one dimension and smaller in the other. The invalidity of contact points on the long ends of the target leads to a grasp which is mostly perpendicular to the longer dimension of the target.

In terms of execution time, the grasp selection procedure takes on average 5.19 seconds without user interaction in an unoptimized python implementation, including the time necessary to create and save multiple figures. Given that the time required for the initialization phase also takes about five seconds, it is reasonable to expect that the manipulation may start within ten seconds from the task definition.

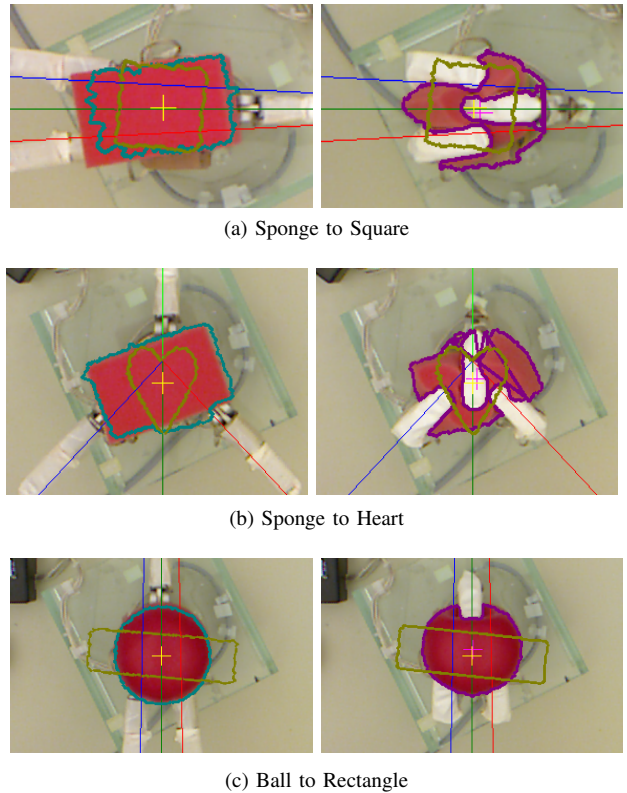


Fig. 12. Sample of results for grasp selection (left) and for the final deformed contour (right), with detected initial object contour in blue, target shape in gold, and final contour in purple. F1 follows the blue line, F2 the red one, and F3 follows the green line from the side where the three lines are the closest ((a) and (c)), or opposite to the red and blue lines (b)

#### V. CONCLUSION

This work proposes an efficient system that integrates RGB-D computer vision with a three-finger robotic gripper for the initial selection of grasping points and 2D shape control of an unknown non-rigid object. By making appropriate use of polar coordinates and various heuristics related to grasp quality and stability, the planner is able to quickly drive the search towards the regions which provide stable grasps that respect the selected robotic hand’s mechanical constraints and facilitate the reshaping task. The resulting algorithm therefore combines the efficiency of a heuristic planner with the accuracy and exhaustivity of a sampling-based one, all without machine learning or formal modelling and simulation of the object. The selected grasp is then combined with real-time object shape tracking and control of the robotic hand to bring the object’s contour closer to the target shape.

Although grasp selection is heavily dependant on the geometry of the robotic hand being used, such that no algorithm can be expected to work for all hand models, the proposed approach eases the transition to other hand geometries by providing general steps that could be reused with little modification. In particular, the identification of regions with a large distance between the contours and the curvature test for stability could be used as-is, while the force closure validation would require some modification to accurately compute the direction of the

applied forces based on the new hand geometry. As long as the fingers close roughly towards the centre of the hand, the simplifications made by using polar coordinates are also expected to work as-is for other hands.

Future directions for this work include validating the selected grasp with a variety of shape control algorithms or building an experimental protocol to better identify the human “intuitive” grasp to use as a benchmark for such reshaping tasks. The system’s flexibility is also expected to be improved by the integration of a robotic arm to control the hand position. In addition, even though the proposed algorithm is reasonably fast and has low requirements in terms of computing power, it is likely that many industrial applications would benefit from increased speed, thus warranting further optimizations.

#### ACKNOWLEDGMENTS

The authors wish to acknowledge support to this research from the Natural Sciences and Engineering Research Council of Canada (NSERC), and from the Ontario Queen Elizabeth II Graduate Scholarship in Science and Technology program.

#### REFERENCES

- [1] J. Sanchez, J.-A. Corrales, B.-C. Bouzgarrou, and Y. Mezouar, “Robotic manipulation and sensing of deformable objects in domestic and industrial applications: A survey,” *The International Journal of Robotics Research*, vol. 37, no. 7, pp. 688–716, Jun. 2018. [Online]. Available: <https://doi.org/10.1177/0278364918779698>
- [2] F. Nadon, A. Valencia, and P. Payeur, “Multi-Modal Sensing and Robotic Manipulation of Non-Rigid Objects: A Survey,” *Robotics*, vol. 7, no. 4, p. 74, Nov. 2018. [Online]. Available: <http://www.mdpi.com/2218-6581/7/4/74>
- [3] F. Nadon and P. Payeur, “Automatic Selection of Grasping Points for Shape Control of Non-Rigid Objects,” in *Proceedings of the IEEE International Symposium on Robotic and Sensors Environments (ROSE)*, Ottawa, ON, Jun. 2019, pp. 170–176.
- [4] K. Shimoga, “Robot Grasp Synthesis Algorithms: A Survey,” *The International Journal of Robotics Research*, vol. 15, no. 3, pp. 230–266, Jun. 1996. [Online]. Available: <https://doi.org/10.1177/027836499601500302>
- [5] T. Yoshikawa, “Multifingered robot hands: Control for grasping and manipulation,” *Annual Reviews in Control*, vol. 34, no. 2, pp. 199–208, Dec. 2010. [Online]. Available: <http://www.sciencedirect.com/science/article/pii/S1367578810000416>
- [6] I.-M. Chen and J. W. Burdick, “Finding antipodal point grasps on irregularly shaped objects,” in *Proceedings - 1992 IEEE International Conference on Robotics and Automation*. IEEE Comput. Soc. Press, 1992.
- [7] Y.-B. Jia, “Curvature-based computation of antipodal grasps,” in *Proceedings - 2002 IEEE International Conference on Robotics and Automation (Cat. No.02CH37292)*, 2002.
- [8] A. Morales, P. J. Sanz, and A. P. del Pobil, “Vision-based computation of three-finger grasps on unknown planar objects,” in *IEEE/RSJ International Conference on Intelligent Robots and System*, 2002.
- [9] R. Suarez, I. Vazquez, and J. M. Ramirez, “Planning four grasping points from images of planar objects,” in *Proceedings of the IEEE International Symposium on Assembly and Task Planning*, 2003.
- [10] A. Herzog, P. Pastor, M. Kalakrishnan, L. Righetti, J. Bohg, T. Asfour, and S. Schaal, “Learning of grasp selection based on shape-templates,” *Autonomous Robots*, vol. 36, no. 1-2, pp. 51–65, Sep. 2013.
- [11] F. Song, Z. Zhao, W. Ge, W. Shang, and S. Cong, “Learning Optimal Grasping Posture of Multi-Fingered Dexterous Hands for Unknown Objects,” in *IEEE International Conference on Robotics and Biomimetics (ROBIO)*, Dec. 2018, pp. 2310–2315.
- [12] J. Xu, A. Bhardwaj, G. Sun, T. Aykut, N. Alt, M. Karimi, and E. Steinbach, “Learning-Based Modular Task-Oriented Grasp Stability Assessment,” in *IEEE/RSJ International Conference on Intelligent Robots and Systems (IROS)*, Oct. 2018, pp. 3468–3475.
- [13] K. Gopalakrishnan and K. Goldberg, “D-space and Deform Closure Grasps of Deformable Parts,” *The International Journal of Robotics Research*, vol. 24, no. 11, pp. 899–910, 2005. [Online]. Available: <https://doi.org/10.1177/0278364905059055>
- [14] D. Mira, A. Delgado, C. M. Mateo, S. T. Puente, F. A. Candelas, and F. Torres, “Study of dexterous robotic grasping for deformable objects manipulation,” in *23rd Mediterranean Conference on Control and Automation (MED)*, Jun. 2015, pp. 262–266.
- [15] L. Zaidi, “Modélisations et stratégie de prise pour la manipulation d’objets déformables,” Ph.D. dissertation, Université Blaise Pascal - Clermont-Ferrand II, Mar. 2016. [Online]. Available: <https://tel.archives-ouvertes.fr/tel-01343377/document>
- [16] L. Zaidi, J. A. Corrales, B. C. Bouzgarrou, Y. Mezouar, and L. Sabourin, “Model-based strategy for grasping 3D deformable objects using a multi-fingered robotic hand,” *Robotics and Autonomous Systems*, vol. 95, pp. 196–206, Sep. 2017. [Online]. Available: <http://www.sciencedirect.com/science/article/pii/S0921889016308089>
- [17] {Barrett Technologies}, “BarrettHand™.” [Online]. Available: <https://advanced.barrett.com/barrethand>
- [18] R. Smeenk, “Kinect V1 and Kinect V2 fields of view compared,” Mar. 2014. [Online]. Available: <https://smeenk.com/kinect-field-of-view-comparison/>
- [19] F. Hui, P. Payeur, and A.-M. Cretu, “Visual Tracking of Deformation and Classification of Non-Rigid Objects with Robot Hand Probing,” *Robotics*, vol. 6, no. 1, p. 5, Mar. 2017. [Online]. Available: <http://www.mdpi.com/2218-6581/6/1/5>
- [20] L. Rocha, L. Velho, and P. C. P. Carvalho, “Image moments-based structuring and tracking of objects,” *Proceedings. XV Brazilian Symposium on Computer Graphics and Image Processing*, pp. 99–105, 2002.
- [21] D. Berenson, “Manipulation of deformable objects without modeling and simulating deformation,” in *IEEE/RSJ International Conference on Intelligent Robots and Systems*, Nov. 2013, pp. 4525–4532.
- [22] A. Morales, G. Recatalá, P. J. Sanz, and A. P. del Pobil, “Heuristic vision-based computation of planar antipodal grasps on unknown objects,” in *Proceedings - IEEE International Conference on Robotics and Automation*, vol. 1, 2001, pp. 583–588.
- [23] P. J. Sanz, J. M. Iñesta, and A. P. del Pobil, “Planar Grasping Characterization Based on Curvature-Symmetry Fusion,” *Applied Intelligence*, vol. 10, no. 1, pp. 25–36, 1999.
- [24] Y. C. Park and G. P. Starr, “Grasp Synthesis of Polygonal Objects Using a Three-Fingered Robot Hand,” *The International Journal of Robotics Research*, vol. 11, no. 3, pp. 163–184, Jun. 1992. [Online]. Available: <https://doi.org/10.1177/027836499201100301>
- [25] F. Nadon, “Sélection de prise et contrôle d’une main robotique pour la manipulation d’objets non rigides,” Thèse de maîtrise, Université d’Ottawa / University of Ottawa, Dec. 2019. [Online]. Available: <http://ruor.uottawa.ca/handle/10393/39995>